Journal of Sound and Vibration (1999) **228**(5), 1145–1165
Article No. jsvi.1999.2495, available online at http://www.idealibrary.com on IDEAL®

VERIFICATION OF LOCAL KRAMERS–KRONIG RELATIONS FOR COMPLEX MODULUS BY MEANS OF FRACTIONAL DERIVATIVE MODEL

T. PRITZ

Acoustics Laboratory, Szikkti Labs, 1034 *Budapest, Bécsi út* 122-124, *Hungary*

(*Received* 7 *September* 1998, *and in final form* 19 *July* 1999)

The local Kramers–Kronig (K–K) relations, which link the damping properties of solid materials at one frequency to the rate of frequency variation of dynamic modulus, are not exact. The validity and accuracy of the local K–K relations is theoretically investigated in this paper by means of material models, especially the fractional Zener model. It is shown that the local K–K relations qualitatively always properly predict the relation between the damping and the frequency dependence of dynamic modulus for any type of deformation and any linear mechanism of energy loss determining the frequency variations. Nevertheless, the accuracy depends on the rate of frequency variation of dynamic properties, mainly of the loss modulus and loss factor, and the weaker the frequency dependence, the better the accuracy. The accuracy is better than 10% if the slope of frequency increase or decrease of loss functions plotted in a log–log system is smaller than 0·35. The application of the local K–K relations to some experimental data is presented.

1. INTRODUCTION

The Kramers–Kronig (K–K) relations have been known from the beginning of this century from the works of Kramers and Kronig who developed them in the theory of electromagnetic wave propagation, and showed that interrelation is between the real and imaginary parts of the complex refraction index [1], and those of the complex susceptibility [2]. After the derivations of Kramers and Kronig, it has been proved that the relations are of general nature, because they are a direct consequence of causality and linearity, which are the features of real linear physical systems. The relations can therefore be used to connect the real and imaginary parts of the relevant frequency response function of systems such as electrical, mechanical and acoustical under certain conditions [3].

The K–K relations can be applied to the complex modulus of elasticity (or its inverse, the complex compliance) [4–8], and are widely used to characterize the linear dynamic properties, dynamic elasticity and damping, of solid materials in the frequency range. The importance and practical usefulness of the relations applied to

0022-460X/99/501145 + 21 $30.00/0

complex modulus is in the fact that they enable one to calculate one dynamic property from the knowledge of the other property versus frequency. Therefore, the K–K relations provide one with a powerful tool for both experimental and theoretical investigations of the complex modulus. For example, the relations may help one to find the proper frequency dependence even if there are large errors in the measured values of one dynamic property, as is common in the case of damping, provided that the experimental data for the other property (the dynamic modulus) versus frequency are "smooth" enough. Notwithstanding, the practical use of the K–K relations is rare [9] because of calculation difficulties. The relations are a pair of integral equation, which in the mathematical context are known as Hilbert transform, and the calculation of integrals is a problem, especially if the variations of dynamic properties are not known for all frequencies from the measurement as is the case usually.

Fortunately, the local versions of the K–K relations are known, which are approximations of the general integral equations [6–8, 10, 11]. The local relations relate the damping properties at one frequency to the rate of frequency variation of dynamic modulus; they are simple and therefore overcome the shortcomings of the integral equations. The disadvantage of the local relations is that they are not exact due to the assumption made in their derivation, namely that the dynamic properties are slowly varying functions of frequency [6, 7]. It is surprising that the accuracy of the local K–K relations theoretically has not been investigated before and, therefore, the limit of the validity has not been cleared in spite of their use in complex modulus measurements [12–15], modelling viscoelastic behaviour [16, p. 94] and in wave propagation studies [6, 17–22].

The essential aim of this paper is to investigate theoretically the validity and accuracy of the local K–K relations with respect to the rate of frequency dependences of dynamic properties. The investigation will be made by means of material models, especially by one of the fractional derivative models, which is able to represent the frequency dependence of dynamic properties of different rates (from linear increase down to the "frequency independence") adequately describing the dynamic behaviour of real solid materials over a wide frequency range [23, 24]. Moreover, the local K–K relations will be applied to some experimental data to demonstrate their applicability and support the results of the theoretical investigation.

2. KRAMERS–KRONIG RELATIONS FOR COMPLEX MODULUS

2.1. GENERAL DEFINITION OF COMPLEX MODULUS

The most general relation between dynamic stress and strain in the linear range of real solid material having both elasticity and damping properties can be given by an integral equation of hereditary type [8], as

$$\sigma(t) = \int_{-\infty}^{t} m(t-\tau)\varepsilon(\tau)\,\mathrm{d}\tau, \tag{1}$$

where $\sigma(t)$ and $\varepsilon(t)$ are the stress- and strain-time history, respectively, t is the time, τ is a dummy variable, $m(t)$ is the memory function:

$$m(t) = \frac{\sigma_m(t)}{\varepsilon_0}, \tag{2}$$

in which $\sigma_m(t)$ is the stress response of material to strain impulse excitation of ε_0 magnitude, i.e., $\varepsilon(t) = \varepsilon_0\, \delta\,(t)$, where $\delta(t)$ is the Dirac delta function. Equation (1) is the mathematical formulation of the Boltzmann superposition principle which is a heuristic one and relies on the linearity. This equation is of general nature, because it is independent of the type of deformation such as shear, compression, etc., and the mechanism of damping, that is the material properties that are involved in the memory function. Until now, equation (1) has been the basis of the phenomenological theory of linear dynamic behaviour of solid materials referred most frequently to as viscoelasticity or anelasticity or sometimes as hereditary elasticity. Furthermore, this equation is formally identical to the fundamental equation of linear systems [3, 8], if $\varepsilon(t)$ is the excitation, i.e., the input function, then $\sigma(t)$ is the output function, the response.

Equation (1) defines the stress to strain ratio in the time domain, where the acoustical or vibrational problems are difficult to solve. One can determine the general equation for the stress to strain ratio in the frequency domain by taking the Fourier transform F of equation (1), provided that the Fourier transform for $\sigma(t)$, $\varepsilon(t)$ and $m(t)$ exist. The Fourier transform for $m(t)$ can be written as

$$\bar{M}(\mathrm{j}\omega) = Fm(t) = \frac{1}{2\pi}\int_{-\infty}^{\infty} m(t)\,\mathrm{e}^{-\mathrm{j}\omega t}\,\mathrm{d}t, \tag{3}$$

where an overbar represents a complex valued function. Applying the transformation rule to the convolution integral, the Fourier transform of equation (1) results in [3]

$$\bar{\sigma}(\mathrm{j}\omega) = \bar{M}(\mathrm{j}\omega)\bar{\varepsilon}(\mathrm{j}\omega). \tag{4}$$

This equation is the complete analogue of the time-domain one (1), therefore equation (4) represents the constitutive law of solid materials in the frequency domain. Furthermore, it is clear that equation (4) represents the Hooke's law generalized for dynamic loading, in which the Fourier transforms of stress- and strain-time histories are linked through a complex quantity $\bar{M}(\mathrm{j}\omega)$ referred to, therefore, as complex modulus of elasticity, which is

$$\bar{M}(\mathrm{j}\omega) = \frac{\bar{\sigma}(\mathrm{j}\omega)}{\bar{\varepsilon}(\mathrm{j}\omega)} = M_d(\omega) + \mathrm{j}M_l(\omega) = M_d(\omega)[1 + \mathrm{j}\eta(\omega)], \tag{5}$$

where M may be any modulus of elasticity (shear, bulk, etc.), M_d is the dynamic modulus of elasticity, M_l is the loss modulus, and η is the loss factor:

$$\eta(\omega) = \frac{M_l(\omega)}{M_d(\omega)}. \tag{6}$$

Note that the complex modulus is usually defined for harmonic vibrations by the ratio of complex amplitudes, which is a special case of the general definition given above.

2.2. EXACT KRAMERS–KRONIG RELATIONS

Definition (5) implies that the complex modulus can be interpreted as the frequency response function of a linear system which is the solid material itself. It is known that the real and imaginary parts of the frequency response function of a real physical linear system, under certain conditions, are interrelated [3]. The relations are known as Kramers–Kronig dispersion relations, or shortly as dispersion relations, after the names of the authors who developed them first in theory of electromagnetic wave propagation [1, 2]. Later on it has been proved that the relations are of general nature, because they rely on the basic physical principle of causality besides linearity. For this reason, the K–K relations have found application in many fields of science such as electrical network theory, electrodynamics, acoustic wave propagation, viscoelasticity, structural dynamics, etc. The causality is the feature of real solid materials; therefore, the K–K relations can be applied to connect the dynamic elastic and damping properties in the linear range of material behaviour.

The relations between the real and imaginary parts of complex modulus, i.e., the dynamic and loss moduli, can be derived from equation (1) by taking into account the causality of memory function, namely $m(t) = 0$ for $t < 0$. Earlier Gross [4] and Sermergor [5] made the derivation for the complex modulus using implicitly the causality. Recently, O'Donell *et al.* [6] have derived the K–K relations for the complex compressibility (reciprocal of the complex bulk modulus) directly employing the causality principle. Furthermore, the K–K relations are derivable by applying the Cauchy's integral formula for the complex modulus, which is a complex frequency function [7, 8], and taking into account the consequencies of causality formulated for the frequency domain [7]. As a result of derivations several forms of the dispersion relations are known; here the formulae involving the static modulus M_0 are given [8]:

$$M_d(\omega) = M_0 + \frac{2\omega^2}{\pi} \mathrm{P} \int_0^\infty \frac{M_l(y)/y}{\omega^2 - y^2} \mathrm{d}y, \tag{7}$$

$$M_l(\omega) = -\frac{2\omega}{\pi} \mathrm{P} \int_0^\infty \frac{M_d(y)}{\omega^2 - y^2} \mathrm{d}y, \tag{8}$$

where y is an integration variable and P denotes the principal value of the integrals.

It is clear that in possession of K–K relations it is sufficient to know one dynamic property-frequency function because the other property, in principle, can be calculated. Nevertheless, the application of K–K relations is not frequent at all because of the difficulties in calculating the integrals. On the one hand, the analytical calculation can be made for some simple functions only. On the other hand, the numerical calculations require, in principle, the knowledge of variations of dynamic properties for all frequencies, but they are known in only a limited frequency range of measurement. The numerical calculation can be performed in the latter case too, but then truncation error may distort the results discussed by Kennedy and Tomlinson [9].

2.3. APPROXIMATE, LOCAL KRAMERS–KRONIG RELATIONS

The above problems can be avoided if one uses the simplified, local versions of the K–K relations. The local relations for the complex modulus can be derived from the integral equation (8) by following the procedure described by O'Donell *et al.* [6] for the complex compressibility, which results in

$$M_l(\omega) \approx \frac{\pi}{2}\omega\frac{\mathrm{d}M_d(\omega)}{\mathrm{d}\omega}, \tag{9a}$$

or

$$M_l(\omega) \approx \frac{\pi}{4,6}\frac{\mathrm{d}M_d(\omega)}{\mathrm{d}\,[\log\omega]} \tag{9b}$$

and

$$\eta(\omega) \approx \frac{\pi}{2}\frac{\mathrm{d}[\log M_d(\omega)]}{\mathrm{d}[\log\omega]}. \tag{10}$$

These equations enable one to calculate the loss modulus or loss factor at one frequency from the knowledge of the slope of dynamic modulus-frequency curve at that frequency. Furthermore, by integrating these equations, the rate of frequency variation, that is the dispersion of dynamic modulus in a frequency range, e.g., ω_1 to ω_2, can be calculated: namely,

$$M_d(\omega_2) - M_d(\omega_1) \approx \frac{2}{\pi}\int_{\omega_1}^{\omega_2}\frac{M_l(\omega)}{\omega}\mathrm{d}\omega, \tag{11a}$$

or

$$M_d(\omega_2) - M_d(\omega_1) \approx \frac{4,6}{\pi}\int_{\omega_1}^{\omega_2} M_l(\omega)\mathrm{d}\log\omega \tag{11b}$$

and

$$\log\frac{M_d(\omega_2)}{M_d(\omega_1)} \approx \frac{2}{\pi}\int_{\omega_1}^{\omega_2}\eta(\omega)\,\mathrm{d}\log\omega. \tag{12}$$

Note that by means of the latter equations, one can calculate only the change of dynamic modulus but not the value of modulus itself, in contrast to equations (9a), (9b) and (10), which give the values of loss modulus and loss factor, respectively, themselves. Note further that, although the derivation of the local K–K relations from the general integral equations is relatively new [6], equations (9a), (9b) and (10) have been known in the theory of viscoelasticity for quite a long time as a result of time-domain investigations [10, 11]. Since then the local relations have been referred to in a number of works devoted to viscoelasticity and have been used in evaluating the results of complex modulus measurements [12–15] and in modelling viscoelastic behaviour [16]. Moreover, the local K–K relations play important role in wave propagation studies too [6, 17–22], because they have served as the basis for deriving the local relations between attenuation and velocity dispersion of acoustic waves propagating in unbounded media [6, 17].

Nevertheless, one has to be cautious when using the local K–K relations for calculations, because they are not exact. The essential reason for inaccuracy of the relations is the assumption used in their derivation, namely that the dynamic properties are slowly varying functions of frequency [6, 7]. The local K–K relations were experimentally verified by Booji and Thoone [7] for the complex shear modulus of a polyvinylacetate sample in a wide frequency range (10^{-8}–10^{2} Hz), and their investigation demonstrates that the inaccuracy increases with the increase of slope of the loss property-frequency function. The experimental verification has not made it possible, of course, for Booji and Thoone to determine the accuracy of the relations analytically. The same applies to the works of O'Donell *et al.* [6] and Lee *et al.* [20] who also experimentally verified the wave version of local K–K relations in a narrow range of ultrasonic frequencies (approx. 0.5–10 MHz) for polyethylene and polyurethane samples respectively. Note that there exist more refined approximations of the general K–K relations [25], that are more accurate than the above local relations, but are more complicated and, therefore, have not found application.

Today it is quite well known that the dynamic behaviour of real solid materials can be adequately described by fractional derivative models [23, 24]. Of these models, the fractional Zener model is especially useful to describe frequency variations of different rates over a wide frequency range. The other advantage of the model is that it satisfies the exact K–K relations. In what follows, this fractional derivative model will be used to investigate the accuracy and validity of the local K–K relations with respect to the rate of frequency variations of dynamic properties. For the sake of completeness, the investigations will start using the original Zener model representing the classical viscoelastic behaviour.

3. VERIFICATION OF LOCAL KRAMERS–KRONIG RELATIONS

3.1. VERIFICATION BY ZENER MODEL

The Zener model also known as a standard linear solid, or standard viscoelastic body or standard anelastic body, is the simplest material model which is able to describe, at least qualitatively, the basic characteristics of dynamic behaviour of real solids, especially the polymeric materials. The model can be represented by two springs and one viscous dashpot as shown in Figure 1. The σ–ε relation describing the model behaviour is a differential equation introduced by Zener [26]:

$$\sigma(t) + \tau_r \frac{\mathrm{d}\sigma(t)}{\mathrm{d}t} = M_0 \varepsilon(t) + M_\infty \tau_r \frac{\mathrm{d}\varepsilon(t)}{\mathrm{d}t}, \tag{13}$$

where τ_r is the relaxation time,

$$\tau_r = \frac{\mu}{M_1}, \tag{14}$$

and μ is the dashpot viscosity, M_1 and M_0 are spring constants; furthermore

$$M_\infty = M_0 + M_1. \tag{15}$$

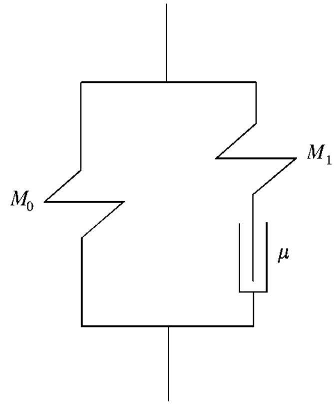

Figure 1. The Zener model.

The complex modulus of the Zener model is derived from equation (13):

$$\bar{M}(j\omega) = \frac{M_0 + M_\infty j\omega\tau_r}{1 + j\omega\tau_r}, \tag{16}$$

from which one can easily determine the dynamic and loss moduli, which are given here in normalized form for the sake of convenience of numerical investigation:

$$\frac{M_d(\omega)}{M_0} = \frac{1 + c\omega_n^2}{1 + \omega_n^2}, \tag{17}$$

$$\frac{M_l(\omega)}{M_0} = \frac{(c-1)\omega_n}{1 + \omega_n^2} \tag{18}$$

and

$$\eta(\omega) = \frac{(c-1)\omega_n}{1 + c\omega_n^2}, \tag{19}$$

where ω_n is the normalized frequency, defined as

$$\omega_n = \omega\tau_r \tag{20}$$

and

$$c = \frac{M_\infty}{M_0}. \tag{21}$$

Figures 2(a) and 2(b) illustrate the variations of these functions in a log–log system for $c = 10$ and 10^3, respectively, in a frequency range covering 12 decades (solid line). It can be seen that the dynamic modulus increases monotonically from M_0, which is the static modulus of elasticity, up to M_∞. The loss functions are zero at zero frequency, and both approach zero at high frequencies after passing through one maximum. The maximum in the loss modulus occurs at normalized frequency

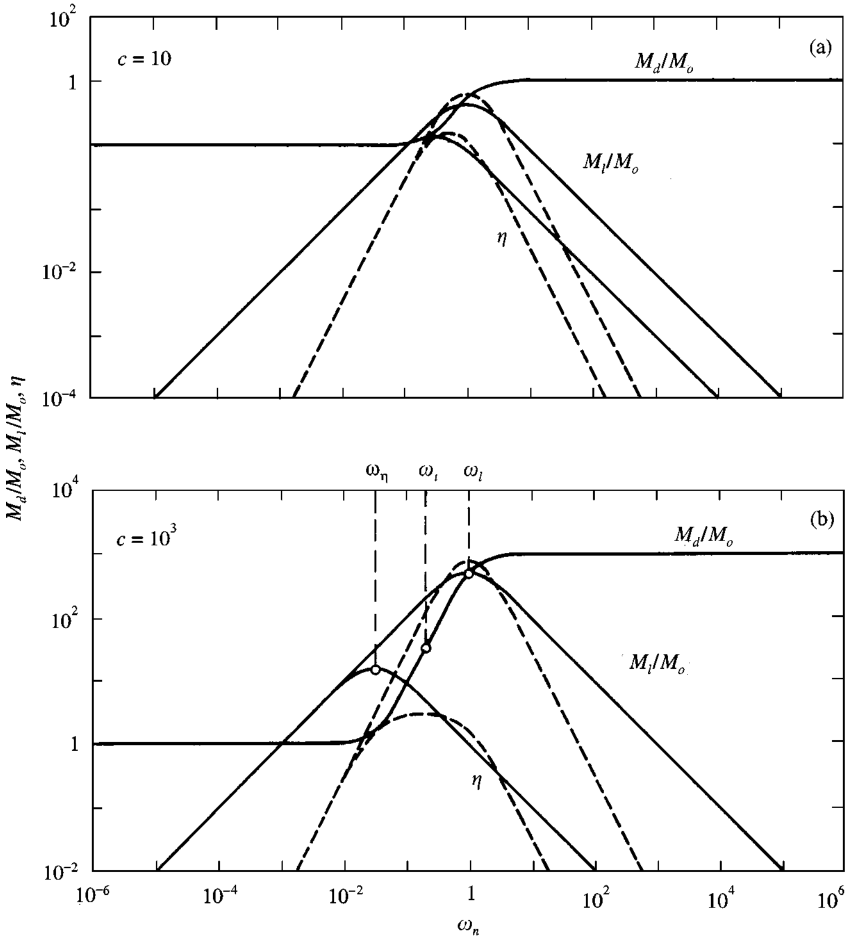

Figure 2. Dynamic modulus, loss modulus and loss factor as functions of normalized frequency. ——, Calculated by the Zener model; – – –, loss properties calculated by the local K–K relations from the dispersion of dynamic modulus.

of $\omega_n = 1 = \omega_l$, and the maximum value M_m normalized to M_0 is

$$\frac{M_m}{M_0} = \frac{c-1}{2}. \tag{22}$$

The frequency of maximum in the loss factor occurs below the maximum in the loss modulus, and depends on c, namely,

$$\omega_\eta = \frac{1}{\sqrt{c}} \leqslant \omega_l, \tag{23}$$

and the maximum loss factor η_m is

$$\eta_m = \frac{c-1}{2\sqrt{c}}. \tag{24}$$

Furthermore, it can be read from equations (18) and (19) that both loss functions increase and decrease linearly and reciprocally with increasing frequency below and above their maximum, respectively; thus the slope of frequency increase and decrease is unity in a log–log system. This slope is independent of the loss peak, and it is a direct consequence of the assumption of Zener model that the energy dissipation can be attributed to the viscosity like fluids. In contrast to the loss functions, the slope of frequency increase of dynamic modulus depends on the loss maximum, i.e., the value of c. The slope of the $\log M_d$–$\log\omega$ function is the largest at the inflection point ω_i, which is

$$\omega_i = \frac{1}{\sqrt[4]{c}} = \omega_\eta \sqrt[4]{c} \geqslant \omega_\eta, \tag{25}$$

therefore ω_i is between the loss peaks,

$$\omega_\eta \leqslant \omega_i \leqslant \omega_l. \tag{26}$$

These frequencies are marked in Figure 2(b) by way of example. The slope s_i at ω_i is

$$s_i = \left.\frac{\mathrm{d}[\log M_d]}{\mathrm{d}[\log\omega]}\right|_{\omega_i} = \frac{2(c-1)\sqrt{c}}{(1+\sqrt{c})(c+\sqrt{c})}. \tag{27}$$

This slope is evidently zero in the case of ideal elasticity ($\eta_m = 0$, $c = 1$), and it can be larger than unity; one has the largest slope if $c \to \infty$, i.e., $\eta_m \to \infty$, then $s_i = 2$. In our examples, $s_i = 1{\cdot}039$ if $c = 10$ ($\eta_m = 1{\cdot}423$), and $s_i = 1.877$ if $c = 10^3$ ($\eta_m = 15.79$).

It can be proved by either an analytical or numerical study that the frequency functions (17) and (18) satisfy the exact K–K relations applied for complex modulus. Therefore, the Zener model can be used to investigate the accuracy of the approximate K–K relations. The investigation can be made by calculating either the loss functions from the frequency dependence of dynamic modulus, or the dispersion of dynamic modulus from the loss functions. Here the loss functions are calculated, because it is the most frequently needed when one interprets the results of measurement of complex modulus. The application of equation (9a) to equation (17) results in

$$\frac{M_l'(\omega)}{M_0} = \frac{\pi(c-1)\omega_n^2}{(1+\omega_n^2)^2} \tag{28}$$

and

$$\eta'(\omega) = \frac{\pi(c-1)\omega_n^2}{(1+c\omega_n^2)(1+\omega_n^2)}, \tag{29}$$

where the accent mark refers to the approximate values. The variations of these functions are drawn in Figure 2 with dashed lines as a function of normalized frequency for $c = 10$ and 10^3 as before. It can be seen that although the characteristics of the approximate and exact loss functions are the same, the values are different with the exception of two intersection points. The difference increases away from the loss peaks, because the approximate loss functions increase and decrease by a function of ω^2 and $1/\omega^2$, respectively, instead of linear frequency increase and reciprocal decrease characterizing the Zener model. Notwithstanding, the frequencies of maxima in the exact and approximate loss moduli coincide but the approximate maximum is larger by 57%, namely,

$$\frac{M'_m}{M_0} = \pi \frac{c-1}{4} = \frac{\pi}{2} \frac{M_m}{M_0}. \tag{30}$$

On the contrary, the frequency of maximum in the approximate loss factor differs from that of the exact one, and occurs at the inflection point of dynamic modulus-frequency curve in accordance with the prediction of equation (10):

$$\omega'_\eta = \omega_i \geqslant \omega_\eta, \tag{31}$$

and here

$$\eta'_m = \pi \frac{c-1}{\sqrt{c}} \frac{c}{(1+\sqrt{c})(c+\sqrt{c})} = \eta_m \frac{2\pi c}{(1+\sqrt{c})(c+\sqrt{c})}. \tag{32}$$

The difference between ω'_η and ω_η, moreover η'_m and η_m, can be especially large if c, i.e., the loss is high, which is seen in Figure 2. For example, if $c = 10^3$ then $\eta'_m = 2{\cdot}949$ and $\omega'_\eta = 0{\cdot}178$ instead of $\eta_m = 15{\cdot}79$ and $\omega_\eta = 0{\cdot}0316$.

As a result of this simple numerical study and bearing in mind that the local K–K relations have been derived under the assumption of slowly varying frequency functions, it can be concluded that the linear frequency increase or reciprocal decrease of loss functions, are too rapid variations for the local relations to yield correct quantitative results. Nevertheless, the qualitative prediction of the local K–K relations is proper even in this case.

3.2. VERIFICATION BY FRACTIONAL ZENER MODEL

It is known that the Zener model, in general is not capable of describing qualitatively the dynamic behaviour of real solid materials. The manifestation of inadequacy of the Zener model in the frequency domain is that the slopes of the theoretical frequency curves plotted in a log–log system is always larger than those of the experimental curves. The behaviour of this model can be improved by decreasing the order of time derivatives in the σ-ε differential equation, i.e., by introducing the so-called fractional derivatives [23]. Therefore, the resulting model, named by the author as the fractional Zener model, has a σ-ε differential equation which is

$$\sigma(t) + \tau_r^\alpha \frac{d^\alpha \sigma(t)}{dt^\alpha} = M_0 \varepsilon(t) + M_\infty \tau_r^\alpha \frac{d^\alpha \varepsilon(t)}{dt^\alpha}, \tag{33}$$

where $0 < \alpha < 1$, and the αth order time derivative of a function, say $\varepsilon(t)$, is defined as [23]

$$\frac{d^\alpha}{dt^\alpha} \varepsilon(t) = \frac{1}{\Gamma(1-\alpha)} \frac{d}{dt} \int_0^t \frac{\varepsilon(\tau)}{(t-\tau)^\alpha} d\tau, \tag{34}$$

in which Γ is the gamma function. Note that this model is also known as the four-parameter fractional derivative model after the number of parameters (M_0, M_∞, τ_r and α).

The complex modulus of the fractional Zener model is derived from equation (33) by replacing the operator d^α/dt^α *with* $(j\omega)^\alpha$ [23]:

$$\bar{M}(j\omega) = \frac{M_0 + M_\infty (j\omega\tau_r)^\alpha}{1 + (j\omega\tau_r)^\alpha}. \tag{35}$$

The dynamic and loss moduli are given again in normalized forms:

$$\frac{M_d(\omega)}{M_0} = \frac{1 + (c+1)\cos(\alpha\pi/2)\omega_n^\alpha + c\omega_n^{2\alpha}}{1 + 2\cos(\alpha\pi/2)\omega_n^\alpha + \omega_n^{2\alpha}}, \tag{36}$$

$$\frac{M_l(\omega)}{M_0} = \frac{(c-1)\sin(\alpha\pi/2)\omega_n^\alpha}{1 + 2\cos(\alpha\pi/2)\omega_n^\alpha + \omega_n^{2\alpha}}, \tag{37}$$

and

$$\eta(\omega) = \frac{(c-1)\sin(\alpha\pi/2)\omega_n^\alpha}{1 + (c+1)\cos(\alpha\pi/2)\omega_n^\alpha + c\omega_n^{2\alpha}}, \tag{38}$$

where ω_n and c are defined as before by equations (20) and (21) respectively.

It can be seen that the introduction of fractional order time derivatives into the σ-ε differential equation results in power functions with α power smaller than unity in the complex modulus-frequency function. Hence, in this way, frequency functions with slopes smaller the unity can be generated. By way of example the frequency curves calculated with $\alpha = 0{\cdot}7$ and $0{\cdot}5$ are drawn in Figures 3 and 4 respectively for $c = 10$ and 10^3 in a frequency range used before (solid line). It can be seen that the characters of frequency dependences of dynamic properties are the same as those of the original Zener model, but the slopes of all frequency curves are smaller; and the smaller the slopes, the smaller the α. Furthermore, it can be read from Figures 3 and 4, and from equations (37) and (38) that the frequency increase and decrease of the loss properties obey a power function of ω_n^α and $1/\omega_n^\alpha$, respectively, at frequencies far enough from the loss maxima. The maximum in the loss modulus occurs at $\omega_n = 1$, and the maximum in the loss factor precedes it, namely,

$$\omega_\eta = \frac{1}{\sqrt[2\alpha]{c}}. \tag{39}$$

The maximum values of the loss functions are

$$\frac{M_m}{M_0} = \frac{c-1}{2}\,\frac{\sin(\alpha\pi/2)}{1 + \cos(\alpha\pi/2)} \tag{40}$$

and

$$\eta_m = \frac{c-1}{2\sqrt{c}}\,\frac{\sin(\alpha\pi/2)}{1 + \dfrac{c+1}{2\sqrt{c}}\cos(\alpha\pi/2)}. \tag{41}$$

The last equation can be simplified as

$$\eta_m \approx \mathrm{tg}(\alpha\pi/2), \tag{42}$$

provided that

$$c \gg \left[\frac{2}{\cos(\alpha\pi/2)}\right]^2, \tag{43}$$

which is satisfied, e.g., for $c > 100$ if $\alpha < 0{\cdot}5$. Furthermore, it can be read from Figures 3 and 4 that the inflection point of the dynamic modulus-frequency curve lies somewhere between the loss peaks as in the original model. The slope of the frequency increase of dynamic modulus at the inflection point is, in general, different from that of the loss functions, and the slope increases with the increase of c, i.e., the loss peak, and decreases with the decrease of α. The computer-generated

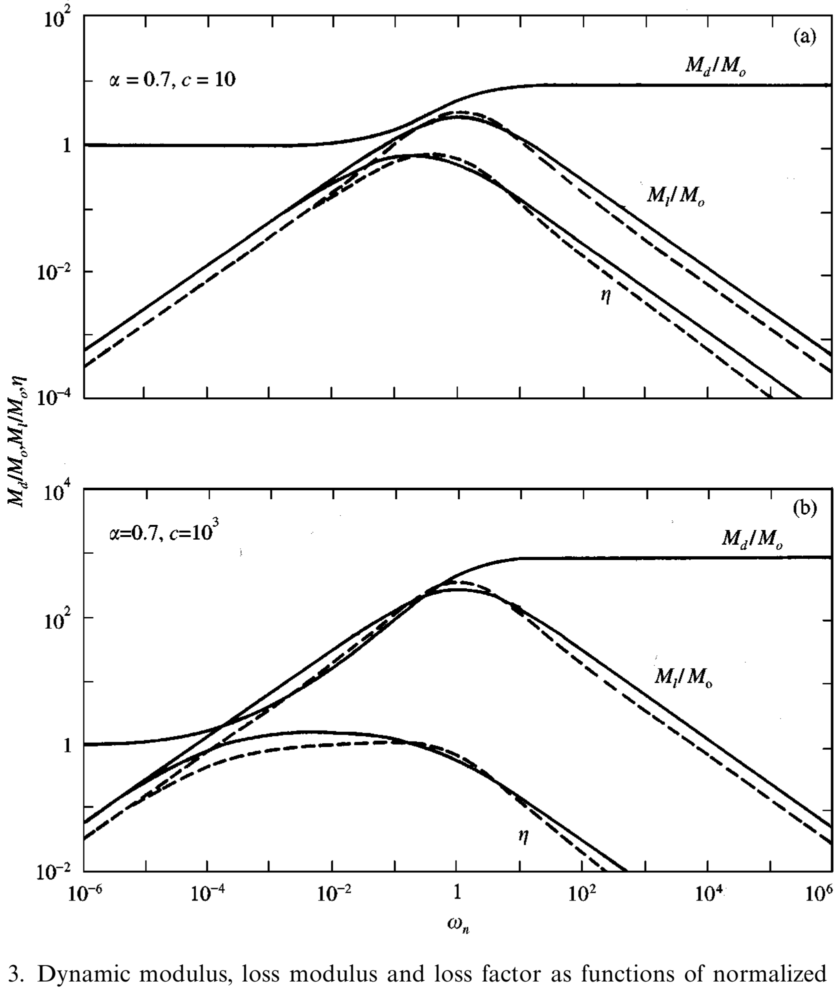

Figure 3. Dynamic modulus, loss modulus and loss factor as functions of normalized freuency. ——, Calculated by the fractional Zener model with $\alpha = 0{\cdot}7$; – – –, loss properties calculated by the local K–K relations from the dispersion of dynamic modulus.

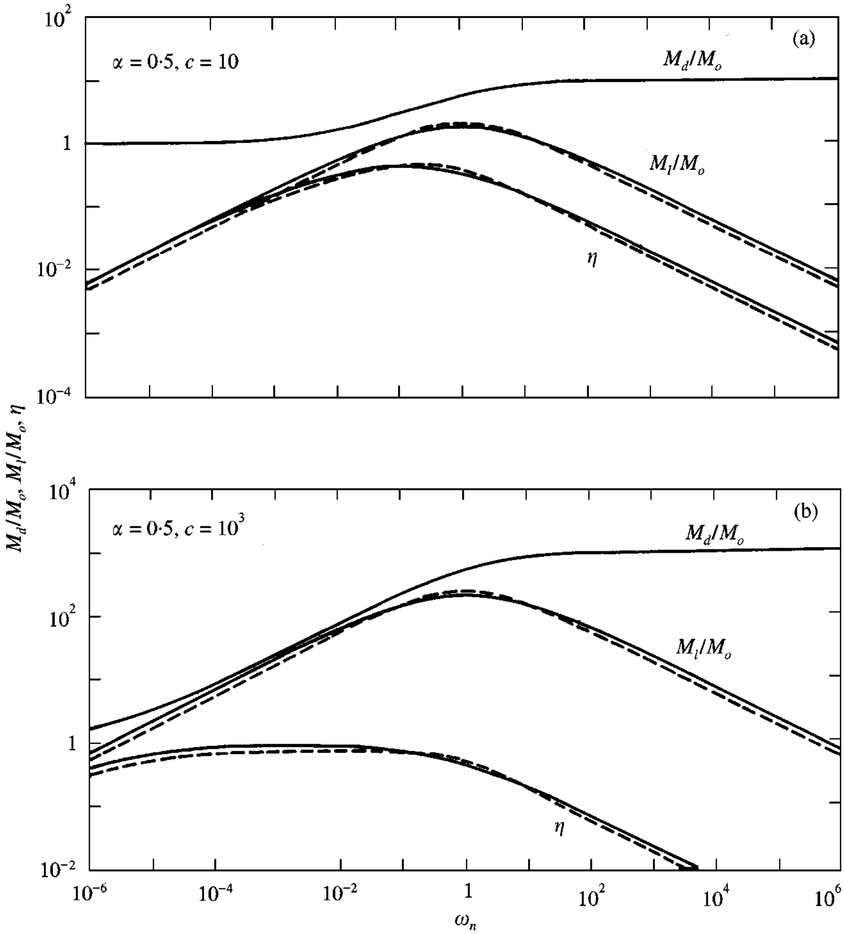

Figure 4. Dynamic modulus, loss modulus and loss factor as functions of normalized frequency. ——, Calculated by the fractional Zener model with $\alpha = 0{\cdot}5$; – – –, loss properties calculated by the local K–K relations from the dispersion of dynamic modulus.

curves show that the slopes of increase of dynamic modulus and loss properties are almost identical in the cases when $c > 10^3$ $\alpha < 0{\cdot}5$ (see Figure 4(b)).

It can be proved by a numerical study using the Hilbert transform program of Matlab that the fractional Zener model obeys the exact K–K relations. Furthermore, from the foregoing, it is clear that this model enables one to generate frequency functions of different slope, from linear increase down to the "frequency independence", by choosing a proper value for α. Therefore, the fractional Zener model provides one with an excellent tool to investigate the accuracy of the local K–K relations with respect to the rate of frequency variations of dynamic properties.

The investigation was performed again by calculating the loss functions from the dynamic modulus-frequency function by means of equations (9) and (10). All calculations were made only numerically in this case to avoid the cumbersome analytic derivations. The parameters of $\alpha = 0{\cdot}9$, $0{\cdot}8$, … , $0{\cdot}1$, and $c = 10$, 10^2 and 10^3 were used for the numerical investigation. The frequency curves calculated with $\alpha = 0{\cdot}7$ and $0{\cdot}5$ for $c = 10$ and 10^3, are shown in Figures 3 and 4, respectively, by way of example (dashed line). It can be seen that although the characteristics of the approximate loss functions are in accordance with those of the exact functions, the values are different. The smaller the α, that is the rate of frequency dependences of dynamic properties, the smaller the difference, i.e. the better the accuracy of the local K–K relations. The inaccuracy is unacceptable if $\alpha > 0{\cdot}7$; considerable improvement starts from $\alpha = 0{\cdot}5$, and no difference can be seen between the exact and approximate frequency curves if $\alpha < 0{\cdot}3$.

3.3. ESTIMATION OF ACCURACY

It can be seen on the frequency curves of Figures 3 and 4 that the difference between the exact and approximate loss functions is the largest far-off from their maxima. Therefore, the accuracy of the local K–K relations can be estimated by calculating the difference between the loss functions at these frequencies. The calculation can be simplified if one recognizes that the increase and decrease of the approximate loss functions, under certain conditions, obey frequency functions of about the same type as that of the exact ones. This statement can be proved by approximating equations (36)–(38), e.g., for low frequencies which are far-off from the loss peak. If one assumes that $\omega_n^\alpha \ll 1$ and $c \gg 1$, then the above equations can be replaced with

$$\frac{M_d(\omega)}{M_0} \approx 1 + c\cos(\alpha\pi/2)\omega_n^\alpha, \tag{44}$$

$$\frac{M_l(\omega)}{M_0} \approx c\sin(\alpha\pi/2)\omega_n^\alpha, \tag{45}$$

and

$$\eta(\omega) \approx \frac{c\sin(\alpha\pi/2)\omega_n^\alpha}{1 + c\cos(\alpha\pi/2)\omega_n^\alpha}. \tag{46}$$

The application of local K–K relation (9a) to equation (44) results in

$$M_l'(\omega) \approx c(\alpha\pi/2)\cos(\alpha\pi/2)\omega_n^\alpha \tag{47}$$

and

$$\eta'(\omega) \approx \frac{c(\alpha\pi/2)\cos(\alpha\pi/2)\omega_n^\alpha}{1 + c\cdot\cos(\alpha\pi/2)\omega_n^\alpha}. \tag{48}$$

The comparison of equations (47) and (48) with equations (45) and (46), respectively, proves the above statement.

The accuracy of the local K–K relations is characterized by the ratio of the approximate and exact loss functions, namely,

$$\frac{M_l'(\omega)}{M_l(\omega)} = \frac{\eta'(\omega)}{\eta(\omega)} = \frac{\alpha\pi/2}{\mathrm{tg}(\alpha\pi/2)} = g(\alpha). \tag{49}$$

The variation of $g(\alpha)$ is plotted in Figure 5. It can be read from this figure that the difference between the exact and approximate values of loss functions is smaller than 10% if $\alpha < 0{\cdot}35$.

Note that the computer-generated curves indicate that the inaccuracy of the local K–K relations is due rather to the frequency variations of loss property than to that of dynamic modulus. In order to verify this observation, frequency curves have been calculated with the assumption of low loss when the frequency dependence of dynamic modulus is negligible ($c \approx 1$). The exact and approximate loss functions calculated with $\eta_m = 0{\cdot}01$ for $\alpha = 1{\cdot}0$ ($c = 1{\cdot}021$) and $\alpha = 0{\cdot}5$ ($c = 1{\cdot}049$) are shown in Figure 6 by way of example. One can see by comparing Figure 6 with Figures 3 and 4 that the differences between the exact and approximate loss functions are about the same regardless of the rate of frequency variations of dynamic modulus, and this supports the above observation. Furthermore, the comparison of these figures disproves a belief frequently referred to in the literature that low loss is required for the validity and accuracy of local K–K relationships besides the slow frequency variations. In all the figures, with the exception of Figure 6, the loss is rather high than low, η_m is around 1·0, and the local K–K relations yield accurate results if the frequency variations of dynamic properties is slow enough.

Note further that the numerical study does not support the prediction of equation (10) that the loss factor peak should occur at the inflection point of the dynamic modulus-frequency curve plotted in a log–log system. In contrast to it, all

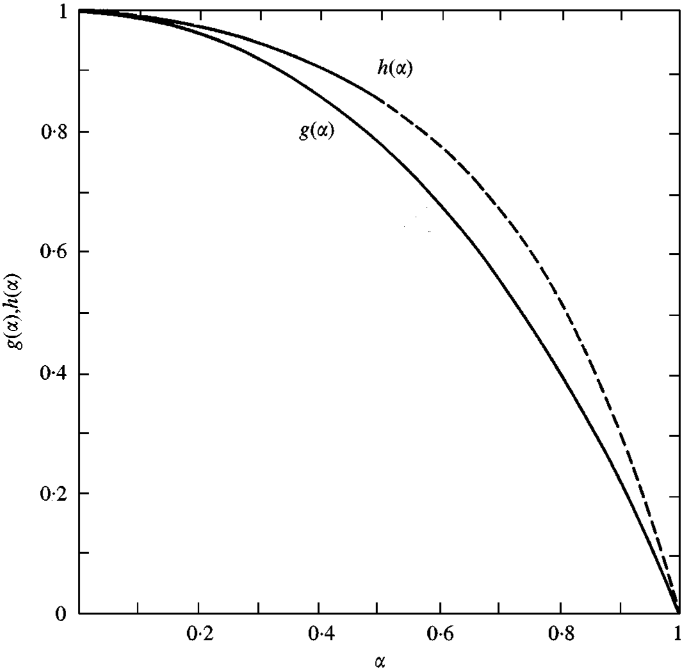

Figure 5. Functions $g(\alpha)$ and $h(\alpha)$ characterizing the accuracy of local K–K relations as functions of α remote from and around the loss factor peak respectively.

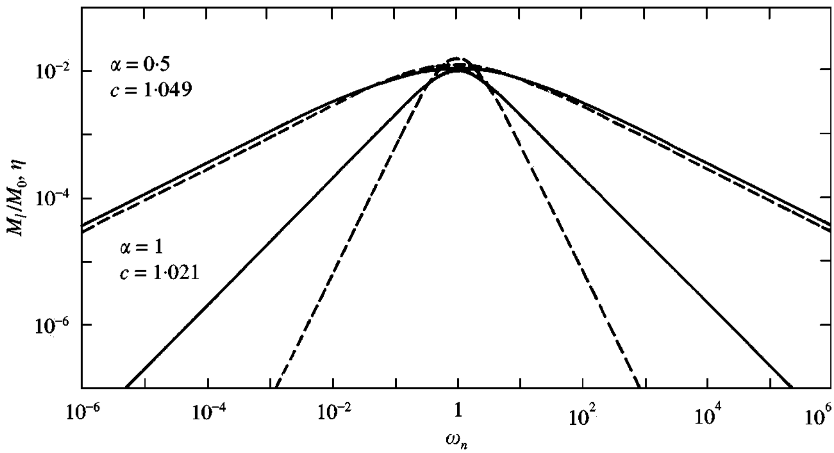

Figure 6. Loss modulus and loss factor as functions of normalized frequency. ——, Calculated by the Zener model ($\alpha = 1$) and the fractional Zener model ($\alpha = 0{\cdot}5$) with the assumption of $\eta_m = 0{\cdot}01$; – – –, calculated by the local K–K relations from the dispersion of dynamic modulus.

theoretical frequency curves show that the loss factor peak occurs below the inflection point, somewhere in the proximity of the lower elbow of the $\log M_d$–$\log\omega$ curve. Notwithstanding, it can be seen on the theoretical frequency curves of Figures 3 and 4 that the inaccuracy of loss factor calculated by the local K–K relation is smaller at and around the loss peak than it is at other frequencies. It can easily be proved if one assumes that $\alpha < 0{\cdot}5$ and $c > 10^3$, when equation (42) holds true and the slope of increase of $\log M_d$–$\log\omega$ curve at the inflection point approximately equals to $\mathrm{tg}\,\alpha$, as mentioned before; therefore

$$\eta'_m \approx \frac{\pi}{2}\frac{\mathrm{d}[\log M_d]}{\mathrm{d}[\log\omega]} \approx \frac{\pi}{2}\mathrm{tg}\alpha. \tag{50}$$

The ratio of equation (50) to equation (42) results in

$$\frac{\eta'_m}{\eta_m} \approx \frac{\mathrm{tg}\alpha(\pi/2)}{\mathrm{tg}(\alpha\pi/2)} = h(\alpha). \tag{51}$$

The comparison of the values of $h(\alpha)$ given in Figure 5, with the values of $g(\alpha)$, supports the above observation. Furthermore, the fact that the inaccuracy is the smallest at and around the loss factor peak, where its frequency variation is the slowest, supports the primary role of frequency variation of loss properties in the accuracy of local K–K relations, as mentioned before.

As a result of this investigation it can be concluded that the accuracy of the local K–K relations applied for the complex modulus is better than 10% at any frequency if the slope of increase or decrease of loss properties–frequency functions plotted in a log–log system is smaller than 0·35. Note that one would arrive at the same conclusion by calculating the dispersion of dynamic modulus from the knowledge of loss properties.

4. APPLICATION TO EXPERIMENTAL DATA

In order to support the conclusions of the theoretical investigation presented above, the local K–K relations have been applied to some experimental data. These data are the dynamic Young's modulus E_d, the relevant loss modulus E_l and the loss factor η_E of a filled rubber (1215 kg/m^3), a polyethylene foam (40 kg/m^3) and a dense PVC foam (450 kg/m^3), which are used for vibration control. The dynamic properties have been measured in the audio frequency range by methods described in references [27] (rubber), [28] (PVC foam) and [29] (polyethylene foam). The measured values of dynamic Young's modulus, loss modulus and loss factor are given in Figures 7–9. Moreover, the frequency dependence of dynamic Young's modulus determined by a curve-fitting method (solid line), and the loss properties calculated by the local K–K relations from the dispersion of dynamic modulus (dashed lines) are given in the figures.

The experimental data for the rubber and the polyethylene foam suggest that the dynamic behaviour of these materials obey frequency functions of the type (44)–(46); therefore these equations have been used to find the value of α and the frequency dependence of dynamic modulus. It can be seen in Figure 7 that the loss properties of the rubber calculated by the local K–K relations from the dispersion of dynamic modulus with $\alpha = 0{\cdot}495$, are underestimated. The inaccuracy is about 20%, which, according to the theoretical predictions, can be explained by the slope of frequency increase of 0·495 of loss properties. In contrast to the rubber, the values of loss modulus and loss factor of the polyethylene foam calculated by the local K–K relations, agree quite well with the measured data due to the slow frequency variation of loss properties ($\alpha = 0{\cdot}199$). This is in good accordance again with the theoretical prediction.

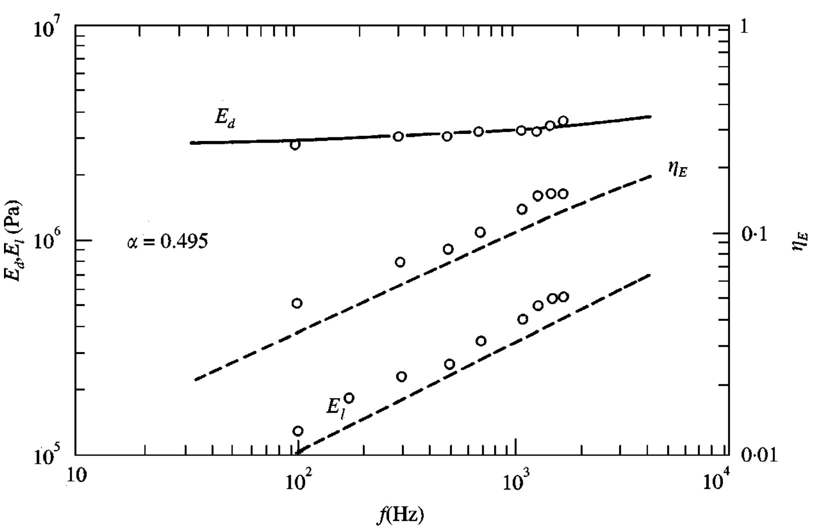

Figure 7. Dynamic Young's modulus, loss modulus and loss factor of a rubber (1215 kg/m^3) plotted against frequency at 25°C. o, Measured values; ——, dynamic modulus determined by curve-fitting method; – – –, loss properties calculated by the local K–K relations from the dispersion of dynamic modulus.

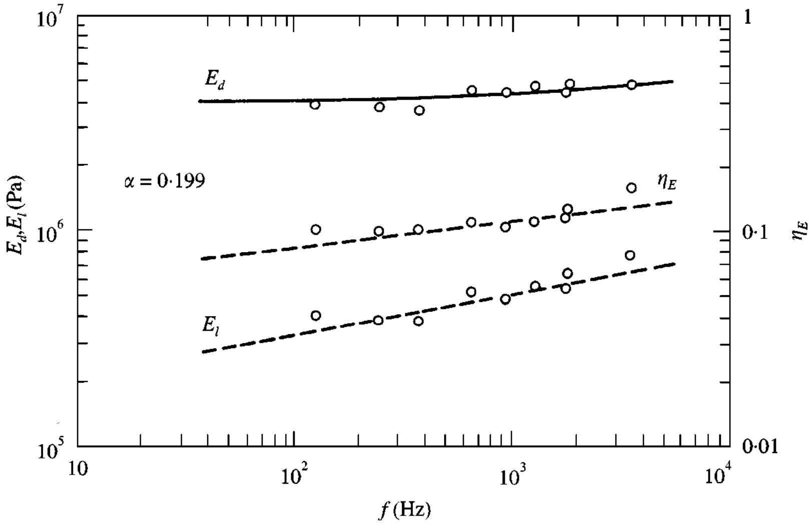

Figure 8. Dynamic Young's modulus, loss modulus and loss factor of a polyethylene foam (40 kg/m^3) plotted against frequency at 24°C. o, Measured values; ——, dynamic modulus determined by curve-fitting method; – – –, loss properties calculated by the local K–K relations from the dispersion of dynamic modulus.

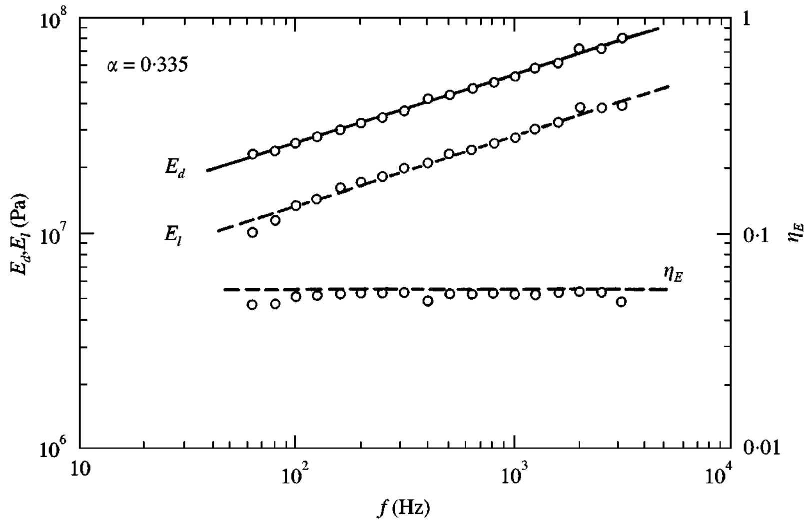

Figure 9. Dynamic Young's modulus, loss modulus and loss factor of a PVC foam (450 kg/m^3) plotted against frequency at 24°C. o, Measured values; ——, dynamic modulus determined by curve-fitting method; – – –, loss properties calculated by the local K–K relations from the dispersion of dynamic modulus.

The loss factor of the PVC foam, in contrast to the above materials, has its maximum value ($\eta_m \approx 0{\cdot}53$) in the frequency range of measurements. It has been proved in an earlier work [24] that the dynamic behaviour of this PVC foam can be described by means of the fractional Zener model over wide frequency range with

$\alpha = 0{\cdot}335$. Furthermore, one can see in Figure 9 that the maximum in the loss factor is flat, and the slopes of frequency increase of dynamic and loss moduli are about identical at these frequencies, like the model behaviour illustrated in Figure 4(b). The maximum value of the loss factor has been calculated with this slope by equation (50), resulting in $\eta'_m \approx 0{\cdot}54$, which agrees very well with the measured values. This agreement supports the theoretical conclusion that the accuracy of local K–K relations is the best at and around the loss peak.

5. CONCLUSIONS

The local K–K relations applied to the complex modulus can be used to calculate the loss modulus and loss factor at one frequency from the rate of frequency variations of dynamic modulus, as can the reverse. The local relations are approximations of the exact K–K integral equations; therefore, they are not accurate. The validity and accuracy of the local K–K relations theoretically has been investigated in this paper with respect to the rate of frequency variations of dynamic properties. As a result of investigation performed by means of the Zener model and the fractional Zener model, the following conclusions can be drawn.

(a) The local K–K relations qualitatively always properly predict the relation between the loss properties and the frequency dependence of dynamic modulus for any type of deformation and any linear mechanism of damping which can be described by a complex modulus. The basic prediction of the relations is that the larger the loss, the larger the frequency increase of dynamic modulus.

(b) The accuracy of the local K–K relations primarily depends on the rate of frequency variation of loss functions; the weaker the frequency variation, the better the accuracy.

(c) The accuracy of the local K–K relations is better than 10% if the slope of freuency increase or decrease of loss functions plotted in a log–log system is smaller than 0·35.

The practical usefulness of the local K–K relations is in that they may help one to interpret, at least qualitatively, the results of measurements of complex moduli for any material regardless of the rate of frequency dependences. One of the important predictions of the local K–K relations is that all dynamic moduli (shear, Young's, etc.) of real materials must increase with increasing frequency. If the frequency dependence measured for a dynamic modulus is weak, then the relevant loss factor is low, otherwise the loss is high and *vice versa*. Furthermore, if the slope of the dynamic modulus-freuency curve plotted in a log–log system increases or decreases, then the loss factor must increase and decrease, respectively, and it pass through a maximum in the proximity of the inflection point of the $\log M_d$–$\log \omega$ curve.

The local K–K relations can be used for evaluating the measured data of complex modulus quantitatively too, provided that the rate of frequency dependences of loss properties satisfy the requirements formulated in (c). Such weak freuency dependences are characteristic of the complex moduli of stiff structural materials (e.g., concrete, wood, etc.), rigid plastics, composites and some plastic foams. On the contrary, the complex moduli of lossy rubbers and polymeric damping materials exhibit strong frequency dependences, when the calculation with the local K–K relations may lead to very inaccurate results.

Note finally that the conclusions drawn here have important consequences for the accuracy of wave version of the local K–K relations applied for lossy, therefore strongly dispersive media, which requires further investigations.

ACKNOWLEDGMENTS

Some of the ideas presented in this paper were born during the author's stay at the Department of Technical Acoustics, Lund Institute of Technology, Sweden. The help of Karl-Ola Lundberg with the application of Hilbert transform program, and the calculation of frequency curves of Figures 2–4 and Figure 6 by Jonas Brunskog, are gratefully acknowledged. The research has been completed with the support of Hungarian Research Fund under contract OTKA, T 019691.

REFERENCES

1. R. de L. Kronig 1926 *Journal of the Optical Society of America* **12**, 547–557. On the theory of the dispersion of X-rays.
2. H. A. Kramers 1927 *Atti del Congresso Internazionale dei Fisíci*, Como, **2**, 545–557. La diffusion de la lumiere par les atomes.
3. D. C. Champeney 1973 *Fourier Transforms and their Physical Applications*. London: Academic Press.
4. B. Gross 1953 *Mathematical Structure of the Theories of Viscoelasticity*, 27. Paris: Hermann.
5. T. D. Sermergor 1960 *Prikladnaja Matematika i Tekhnicheskaia Fizika* **1**, 96–102. On dispersion relations for elasticity and compliance (in Russian).
6. M. O'Donell, E. T. Jaynes and J. G. Miller 1981 *Journal of the Acoustical Society of America* **69**, 696–701. Kramers–Kronig relationship between ultrasonic attenuation and wave velocity.
7. H. C. Booji and G. P. J. M. Thoone 1982 *Rheologica Acta* **21**, 15–24. Generalization of Kramers–Kronig transforms and some approximations of relations between viscoelastic quantities.
8. N. W. Tschoegl 1989 *The Phenomenological Theory of Linear Viscoelastic Behaviour: An Introduction*. Berlin: Springer.
9. I. Kennedy and G. R. Tomlinson 1988 *Journal of Sound and Vibration* **122**, 149–169. Torsional vibration transmissibility characteristics of reinforced viscoelastic flexible pipes.
10. A. J. Staverman and F. Schwarzl 1956 *Die Physik der Hochpolymeren* (H. A. Stuart, editor) **IV**, 28. Berlin: Springer. Linear deformation behaviour of high polymers.
11. W. Philippov 1965 *Physical Acoustics* (W. P. Mason, editor) **II**, Part B, 27. New York: Academic Press. Relaxations in polymer solutions, liquids, and gels.
12. A. Naemura, T. Kurosaki and M. Tsuchida 1972 *Review of the Electrical Communication Laboratories* **20**, 495–510. Research on dynamic modulus of polymer materials.
13. E. J. Dickinson and H. P. Witt 1974 *Transactions of the Society of Rheology* **18**, 591–606. The dynamic shear modulus of paving asphalts as a function of frequency.
14. B. E. Read and G. D. Dean 1978 *The Determination of Dynamic Properties of Polymers and Composites*, 183. Bristol, U.K.: Adam Hilger.
15. N. Lagakos, J. Jarzynski, J. H. Cole and J. A. Bucaro 1986 *Journal of Applied Physics* **59**, 4017–4031. Frequency and temperature dependence of elastic moduli of polymers.

16. A. D. Nashif, D. I. G. Jones and J. P. Henderson 1985 *Vibration Damping*. New York: Wiley.
17. H. Kolsky 1960 *Proceedings of International Symposium on Stress Wave Propagation in Materials* (N. Davids, editor), 59–90. New York: Interscience. Viscoelastic waves.
18. M. S. Hughes, S. M. Handley and J. G. Miller 1987 *Proceedings of the IEEE Ultrasonics Symposium*, 1041–1045. New York: IEEE Nearly local Kramers–Kronig relations applied to porous epoxy.
19. E. Soczkiewicz 1989 *Proceedings of the* 13*th International Congress on Acoustics, Beograd*, **4**, 269–272. Application of the local Kramers–Kronig relationship to the calculation of the ultrasonic waves attenuation in highly viscous liquids.
20. C. C. Lee, M. Lahham and B. G. Martin 1990 *IEEE Transactions on Ultrasonics, Ferroelectrics, and Frequency Control* **37**, 286–296. Experimental verification of the Kramers–Kronig relationship for acoustic waves.
21. H. Kolsky 1992 *M^3D: Mechanics and Mechanism of Material Damping* (V. K. Kinra, A. Wolfenden, editors), **ASTM STP-1169**, 4–27. The measurement of the material damping of high polymers over ten decades of frequency and its interpretation.
22. T. L. Szabo 1995 *Journal of the Acoustical Society of America* **97**, 14–24. Causal theories and data for acoustic attenuation obeying a frequency power law.
23. P. J. Torvik and R. L. Bagley 1984 *American Society of Mechanical Engineers Journal of Applied Mechanics* **51**, 294–298. On the appearance of the fractional derivate in the behaviour of real materials.
24. T. Pritz 1996 *Journal of Sound and Vibration* **195**, 103–115. Analysis of four-parameter fractional derivate model of real solid materials.
25. A. Brather 1987 *Rheologica Acta* **17**, 325–341. Numerisch einfache Beziehungen zwischen Verlust- und Speicherkomponente des dynamischen Schermodulus und der dynamischen Nachgiebigkeit.
26. C. Zener 1948 *Elasticity and Anelasticity of Metals*, 43. The University of Chicago Press: Chicago.
27. T. Pritz 1980 *Journal of Sound and Vibration* **72**, 317–341. Transfer function method for investigating the complex modulus of acoustic materials: spring-like specimen.
28. T. Pritz 1991 *Proceedings of the* 9*th FASE Symposium and* 10*th Hungarian Conference on Acoustics, Balatonfüred*, 273–276. Dynamic characteristics of PVC foams.
29. T. Pritz 1994 *Journal of Sound and Vibration* **178**, 315–322. Dynamic Young's modulus and loss factor of plastic foams for impact sound isolation.